Proceedings of the ASME 2012 International Mechanical Engineering Congress & Exposition
IMECE2012
November 9-15, 2012, Houston, Texas, USA

IMECE2012-87957

LOW-VARIANCE MONTE CARLO SIMULATION OF THERMAL TRANSPORT IN GRAPHENE

Colin Landon
Department of Mechanical Engineering
Massachusetts Institute of Technology
Cambridge, MA 02139
Email: clandon@mit.edu

Nicolas G. Hadjiconstantinou
Department of Mechanical Engineering
Massachusetts Institute of Technology
Cambridge, MA 02139
Email: ngh@mit.edu

ABSTRACT

Due to its unique thermal properties, graphene has generated considerable interest in the context of thermal management applications. In order to correctly treat heat transfer in this material, while still reaching device-level length and time scales, a kinetic description, such as the Boltzmann transport equation, is typically required. We present a Monte Carlo method for obtaining numerical solutions of this description that dramatically outperforms traditional Monte Carlo approaches by simulating only the deviation from equilibrium. We validate the simulation method using an analytical solution of the Boltzmann equation for long graphene nanoribbons; we also use this result to characterize the error associated with previous approximate solutions of this problem.

INTRODUCTION

Graphene consists of a single layer of sp^2 bonded carbon atoms. The strong bonds impart favorable mechanical, thermal and electrical properties [1, 2], which have resulted in considerable interest in graphene-based devices. In this work, we consider thermal transport in graphene devices, where due to long phonon mean free paths, Fourier-based descriptions are insufficient.

To capture this behavior, we use a semi-classical model based on the phonon Boltzmann equation [3] which treats phonons as classical point particles whose velocity is determined from a quantum-mechanically determined dispersion relation. At boundaries, transmission and reflection phenomena are captured by quantum-based transmission and reflection coefficients. Some other wave-like properties (i.e. interference and coherence) are not captured using this approach. Fortunately, the length scale for which the latter are expected to be important is small compared to the size of typical graphene devices. At room temperature and using the Debye approximation for phonon energy $E = h\nu_D/\lambda$, where h is Planck's constant and $\nu_D \approx 2\times10^4$m/s [4] is the Debye velocity, wave-like phenomena are of the same order as thermal (classical) effects at a length scale of $\mathcal{O}(1\text{nm})$. Thus, for ribbons of widths $W \sim \mathcal{O}(10\text{nm})$ and larger, we expect our semi-classical approach to be applicable.

The high-dimensionality and singularities in the distribution function associated with solutions of the Boltzmann equation [5], as well as complex geometries typically found in engineering problems, make Monte Carlo (MC) methods for solving this equation appealing. Unfortunately, the convergence of Monte Carlo methods with the number of samples is slow, resulting in high statistical uncertainty (noise), that in some cases obscures the phenomenon of interest, particularly for near equilibrium problems [6].

It was recently shown that this limitation can be overcome by "deviational" methods, such at the Low-variance Deviational Simulation Monte Carlo (LVDSMC) [5, 7–9]. By simulating only the deviation from equilibrium, these methods drastically reduce the statistical uncertainty associated with the Monte Carlo sampling process, thereby significantly outperforming traditional Monte Carlo approaches (e.g. [10, 11]).

Nanoribbons are a fundamental component of many graphene-based devices and thus understanding their heat trans-

port properties is of considerable importance. So far, their effective thermal conductivity has been modeled using one of two approximate approaches: the first approach assumes that their finite size imposes a wavelength cut-off above which phonons do not contribute to the heat flux [2, 12–14]; the second approach assumes that the effect of boundaries can be accounted for by augmenting the homogeneous scattering rate [15–17] of the material. In this paper, we use a combination of analytical results and low-variance simulation methods to obtain accurate solutions of the Boltzmann equation for the effective thermal conductivity of graphene nanoribbons with diffusely scattering boundaries. Specifically, we use an analytical solution of the Boltzmann equation for infinitely long graphene nanoribbons to validate our LVDSMC approach and characterize the error associated with the previous approximate approaches.

SIMULATION METHOD

The phonon Boltzmann equation, first formulated by Peierls [3], is an evolution equation for the single-particle distribution function $f = f(t, \mathbf{x}, \mathbf{k}, p)$ where t is the time, $\mathbf{x}$ is the position, $\mathbf{k}$ is the wavevector, and p is the polarization. In what follows, when no ambiguity exists, the functional dependence of the distribution function on all variables will not be explicitly indicated.

In Monte Carlo solution methods, significant computational advantage is gained [5, 7–9] by considering deviations $f^{\mathrm{d}} = f - f^{\mathrm{eq}}$ from a reference equilibrium (Bose-Einstein) distribution $f^{\mathrm{eq}} = f^{\mathrm{BE}}(\omega, T_{\mathrm{eq}}) = \left(\exp\left[(\hbar\omega)/(k_{\mathrm{B}}T_{\mathrm{eq}})\right] - 1\right)^{-1}$ at a *suitably chosen* equilibrium temperature T_{eq}. Although we have written the distribution as a function of the frequency ω, it still depends upon the wave vector through the dispersion relation $\omega = \omega(\mathbf{k}, p)$. Here, we choose to simulate the Boltzmann equation in terms of energy,

$$\frac{\partial \hbar\omega f^{\mathrm{d}}}{\partial t} + \mathbf{v}\cdot\nabla_{\mathbf{x}}\hbar\omega f^{\mathrm{d}} = -\frac{\hbar\omega f^{\mathrm{d}} - \hbar\omega f^{\mathrm{loc,d}}}{\tau(\omega, p, T)}, \tag{1}$$

as recommended in [9]; this improves the energy conservation properties of the algorithm. In our notation, $\mathbf{v} = \mathbf{v}(\mathbf{k}, p) = \nabla_{\mathbf{k}}\omega(\mathbf{k}, p)$ is the phonon group velocity; by subtracting the equilibrium distribution from the local distribution in the collision term, one obtains the local deviational distribution function $f^{\mathrm{loc,d}} = f^{\mathrm{loc}} - f^{\mathrm{eq}}$.

The LVDSMC simulation uses computational particles to represent and sample $\hbar\omega f^{\mathrm{d}}$. For convenience and in accordance with available relaxation times, we assume isotropy and include the density of states (denoted by $D(\omega, p)$ for polarization p) so that the computational particles are a discrete approximation of

$$\begin{aligned}\mathscr{F}(\omega) &= \sum_p \hbar\omega f^{\mathrm{d}}(\omega)\frac{D(\omega,p)}{2\pi} \\ &\approx \mathscr{E}_{\mathrm{eff}}\sum_i S_i\delta^2(\mathbf{x}-\mathbf{x}_i)\delta(\omega-\omega_i)\delta(\theta-\theta_i)\delta_{p,p_i},\end{aligned} \tag{2}$$

where $\mathscr{E}_{\mathrm{eff}}$ is the effective energy carried by each computational particle and S_i is the sign of the particle (+1 or -1 for positive and negative deviations from equilibrium, respectively). Here we have written the distribution function in terms of the frequency ω, which is convenient for readability, but only admissible for one-to-one dispersion relations like the acoustic branches in graphene. In this notational scheme, the group velocity is a function of frequency, angle, and polarization $\mathbf{v} = \mathbf{v}(\omega, \theta, p)$; from which we can write the density of states for an isotropic atomically thin sheet (with thickness δ) as

$$D(\omega, p)\mathrm{d}\omega = \frac{\omega}{2\pi|\mathbf{v}(\omega,\theta,p)|\delta}\mathrm{d}\omega. \tag{3}$$

The dynamic behavior of the computational particles is governed by equation (1). As is typical in Monte Carlo particle methods, integration of this equation utilizes four main algorithmic ingredients: initialization, sampling, advection and scattering. These are discussed below. The details of the implementation are discussed by Péraud and Hadjiconstantinou for three-dimensional phonon simulations [9]. Here we briefly describe the algorithm with particular emphasis on the changes required for simulating a two-dimensional material.

Initialization

Given some isotropic initial condition $f(\omega, t = 0)$, the simulation is started by generating particles from the distribution

$$\mathscr{F}(\omega)\mathrm{d}\omega = \sum_p \hbar\omega\left[f(\omega, t=0) - f^{BE}(\omega, T_{eq})\right]D(\omega, p)\mathrm{d}\omega. \tag{4}$$

Frequently, $f(\omega, t = 0)$ is another equilibrium distribution, either due to the problem definition, or, as is the case here, because the interest lies in the steady state solution of the Boltzmann equation and thus $f(\omega, t = 0)$ can be chosen with convenience in mind. In both cases, if the reference equilibrium temperature is chosen to be the same as the initial equilibrium temperature, the simulation starts with no (deviational) particles in the simulation domain. This approach is adopted here.

Sampling

All properties of interest over some region of space V are calculated by taking moments of the distribution function. In

particular, the energy is given by

$$E = \sum_p \int_{\mathbf{x}\in V} \int_0^{\omega_{p,\max}} \hbar\omega f(\omega) D(\omega, p) \mathrm{d}\omega \mathrm{d}^3\mathbf{x} \tag{5}$$

where $\omega_{p,\max}$ is the upper limit of the dispersion for branch p. In light of Eqn. (2), we decompose this into a deviational part and an equilibrium part

$$\begin{aligned} E &= \int_{\mathbf{x}\in V} \int_0^{\omega_{p,\max}} \mathscr{F}(\omega) \mathrm{d}\omega \mathrm{d}^3\mathbf{x} + E_{\mathrm{eq}}(T_{\mathrm{eq}}) \\ &\approx \mathscr{E}_{\mathrm{eff}} \sum_i S_i + E_{\mathrm{eq}}(T_{\mathrm{eq}}). \end{aligned} \tag{6}$$

The last term in Eqn. (6) can be calculated deterministically (with no stochastic noise) from

$$E_{\mathrm{eq}}(T) = V \sum_p \int_0^{\omega_{p,\max}} \frac{\hbar\omega}{\exp\left(\frac{\hbar\omega}{k_{\mathrm{B}}T}\right) - 1} D(\omega, p) \mathrm{d}\omega. \tag{7}$$

Thereby the computational effort is focused only on the first term, which leads to the dramatic variance-reduction exhibited by LVDSMC simulations. Similarly, the heat flux can be calculated from

$$\begin{aligned} \mathbf{q}'' &= \frac{1}{V} \sum_p \int_{\mathbf{x}\in V} \int_0^{2\pi} \int_0^{\omega_{p,\max}} \mathbf{v} \hbar\omega f(\omega) \frac{D(\omega, p)}{2\pi} \mathrm{d}\omega \mathrm{d}\theta \mathrm{d}^3\mathbf{x} \\ &\approx \frac{\mathscr{E}_{\mathrm{eff}}}{V} \sum_i S_i \mathbf{v}(\omega_i, \theta_i, p_i). \end{aligned} \tag{8}$$

Advection

During the advective step, particles move ballistically according to $\mathbf{x}_i(t + \Delta t) = \mathbf{x}_i(t) + \mathbf{v}_i \Delta t$. When particles encounter boundaries, boundary conditions are imposed by considering the physical interpretation of the associated boundary condition in terms of the deviation from equilibrium. Examples can be found in [9].

Here we discuss the case of a boundary at a fixed temperature T_{w}. In what follows, we will use the notation

$$f^{\mathrm{d}}(\omega; T, \hat{T}) = f^{\mathrm{BE}}(\omega, T) - f^{\mathrm{BE}}(\omega, \hat{T}) \tag{9}$$

to denote the deviational distribution arising from the difference between two equilibrium distributions.

To determine the energy flux at such a boundary, we use the heat flux relation Eqn. (8), which yields

$$q''_{\mathrm{w}} = \sum_p \int_{-\pi/2}^{\pi/2} \int_0^{\omega_{p,\max}} \hbar\omega |\mathbf{v}| \cos(\theta) f^{\mathrm{d}}(\omega; T_{\mathrm{w}}, T_{\mathrm{eq}}) \frac{D(\omega, p)}{2\pi} \mathrm{d}\omega \mathrm{d}\theta, \tag{10}$$

where θ is measured with respect to the boundary normal. Equation (10) allows us to conclude that the distribution from which particle frequencies need to be generated is

$$\mathscr{F}(\omega)\mathrm{d}\omega = \sum_p \hbar\omega |\mathbf{v}| f^{\mathrm{d}}(\omega; T_{\mathrm{w}}, T_{\mathrm{eq}}) D(\omega, p) \mathrm{d}\omega, \tag{11}$$

while the angular distribution follows $P(\theta)\mathrm{d}\theta = \frac{\cos(\theta)}{2}\mathrm{d}\theta$.

The boundary condition just described could be used to apply a temperature gradient along the graphene nanoribbon, but this approach would require explicitly simulating its entire length. For the very long ribbons of interest here, a more convenient approach consists of simulating only a small segment of the ribbon (length L) and subjecting it to a uniform temperature gradient $(T_2 - T_1)/L$, where T_1 and T_2 are the temperatures at the ribbon boundaries in the axial direction (corresponding to the ribbon length). This boundary condition has been developed [11] as a means of calculating the effective thermal conductivity of periodic nanostructures subject to an external temperature gradient. Deviational simulations lend themselves naturally to this type of boundary condition: they can be implemented [9] by applying toroidal boundary conditions to existing particles, while generating new particles at the periodic boundaries. At the boundary at temperature T_1, the particles are drawn from the distribution

$$\mathscr{F}(\omega)\mathrm{d}\omega = \sum_p \hbar\omega |\mathbf{v}| f^{\mathrm{d}}(\omega; T_1, T_2) D(\omega, p) \mathrm{d}\omega, \tag{12}$$

while due to the symmetry inherent in this problem and in order to enforce energy conservation, the same frequencies can be used for the particles generated at the boundary at T_2, provided their signs are reversed $[f^{\mathrm{d}}(\omega; T_1, T_2) = -f^{\mathrm{d}}(\omega; T_2, T_1)]$. The angular distribution of particles follows $P(\theta)\mathrm{d}\theta = \frac{\cos(\theta)}{2}\mathrm{d}\theta$.

Nanoribbon free boundaries are commonly modeled as diffuse adiabatic boundaries: particles incident on the boundary are reflected back into the simulation domain, with an angular distribution given by $P(\theta)\mathrm{d}\theta = \frac{\cos(\theta)}{2}\mathrm{d}\theta$.

Scattering

In the scattering step, particles are selected proportionally to their scattering probability $P(\omega_i, p_i, T_{\mathrm{loc}}) = 1 - \exp[-\Delta t/\tau(\omega_i, p_i, T_{\mathrm{loc}})]$ for deletion. The local temperature T_{loc} is determined by computing the local energy E_{loc} with Eqn. (6) and then by numerically inverting Eqn. (7).

After particle deletion, new particles are generated to drive the simulation towards the local equilibrium, f^{loc}, a Bose-Einstein distribution at the scattering pseudo-temperature, T_{s}.

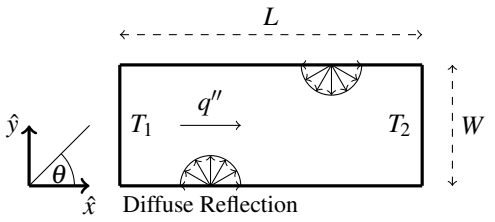

FIGURE 1. SCHEMATIC OF NANORIBBON OF GRAPHENE WITH DIFFUSE BOUNDARIES

The latter is defined such that

$$\sum_p \int_0^{\omega_{p,\max}} \frac{\hbar\omega f^{\mathrm{BE}}(\omega,T_\mathrm{s})}{\tau(\omega,p,T_\mathrm{loc})} D(\omega,p)\mathrm{d}\omega = \sum_p \int_0^{\omega_{p,\max}} \frac{\hbar\omega f(\omega)}{\tau(\omega,p,T_\mathrm{loc})} D(\omega,p)\mathrm{d}\omega, \tag{13}$$

which enforces energy conservation during scattering. The pseudo-temperature is calculated by numerically inverting Eqn. (13) whose right-hand-side can be evaluated from simulation data. The total number of new particles to draw and their associated sign is determined by the sum of the signs of deleted particles; the new particles are drawn from

$$\mathscr{F}(\omega)\mathrm{d}\omega = \sum_p \hbar\omega \frac{f^\mathrm{d}(\omega;T_\mathrm{s},T_\mathrm{eq})}{\tau(\omega,p,T_\mathrm{loc})} D(\omega,p)\mathrm{d}\omega. \tag{14}$$

According to our notation, $f^\mathrm{d}(\omega;T_\mathrm{s},T_\mathrm{eq}) = f^{\mathrm{loc,d}}$ from Eqn. (1).

MATERIAL MODEL

In this section, we focus our discussion by specifying our choice of phonon dispersion relation and relaxation times. The calculations in this work will be for near room temperature isotopically pure graphene with no point defects, strain, or grain boundaries. We use the phonon dispersion calculated from density functional theory (Quantum-Espresso) according to the parameters given by Mounet [18]. Due to our assumption of isotropy, we must choose a single direction in the hexagonal Brillouin zone; here, we chose $\Gamma = [0,0]$ to $K = [\frac{4\pi}{3a},0]$. For relaxation times, we use a Debye-Callaway-like model [15, 19] following the adaptation for graphene from Aksamija [17], which agreed with experimentally measured heat fluxes. Normal scattering is neglected; the umklapp scattering rate is approximately given by [19]

$$\tau(\omega,p,T)^{-1} \approx \frac{\hbar\gamma_p^2}{M\Theta_p\bar{v}_p^2}\omega^2 T\exp(-\Theta_p/3T), \tag{15}$$

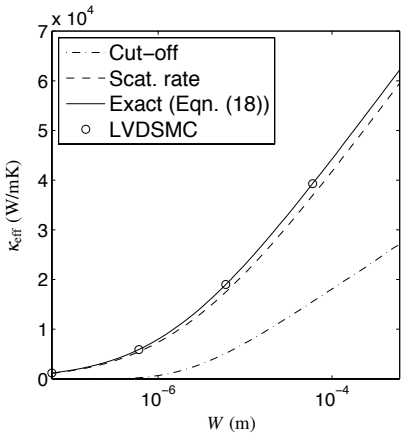

FIGURE 2. EFFECTIVE CONDUCTIVITY OF LONG GRAPHENE NANORIBBONS AS A FUNCTION OF WIDTH. COMPARISON OF VARIOUS METHODS.

where M is the average atomic mass, $\bar{v}_p$ is the speed of sound (the slope of the dispersion relation near the Γ point) for branch p, γ_p is the Grüneisen parameter for branch p which has the value of 0.7 for the transverse acoustic branch and 1.8 for the longitudinal acoustic branch [18], and Θ_p is the branch specific Debye temperature obtained from [17]

$$\Theta_p^2 = \frac{5\hbar^2}{3k_\mathrm{B}^2}\frac{\int\omega(k,p)^2 k\mathrm{d}k}{\int k\mathrm{d}k}. \tag{16}$$

Near room temperature, the out-of-plane branches can be neglected, due to their large Grüneisen parameter and small group velocity. The optical branches are also neglected due to their small group velocity. In other words, here we use a two branch model (TA and LA) with DFT calculated dispersion relations coupled to the empirical relaxation time model.

LONG GRAPHENE NANORIBBONS

In this section we discuss the effective thermal conductivity, $\kappa_{\mathrm{eff}} = q''L/(\Delta T)$, of long graphene nanoribbons. The geometry and associated nomenclature is shown in Fig. 1. Finite length nanoribbons will be discussed in a future publication [20].

Even before the first isolation of graphene flakes, Klemens recognized that two-dimensional structures would have unique thermal transport characteristics. Specifically, the thermal conductivity is only finite for finite sized graphene samples [12] and is thus a *device* property and not a material property. To capture this size-effect, Klemens formulated a cut-off frequency by assuming that "the [phonon] mean free path cannot exceed the smallest linear dimension of the sheet." This approach leads to an effective thermal conductivity that increases with increasing

ribbon width [13], but is significantly different from the analytical solution of the Boltzmann equation discussed below. From a kinetic theory point of view, this is expected, since phonons with mean free paths longer than the size of the graphene ribbon still contribute to heat transfer, albeit ballistically. To quantify the error associated with Klemens' approach and compare with other methods, we calculate the frequency-dependent mean free path $\Lambda(\omega,p)=\tau(\omega,p,T)|\mathbf{v}(\omega,p)|$ and cut off all contributions to the heat flux with $\Lambda > W$. The results at $T = 300$K are shown in Fig. 2 and are labeled "Cut-off."

Our results show that adding a (homogeneous) scattering rate to the intrinsic (phonon-phonon) scattering rate in Eqn. (15) as a means of capturing the effect of boundaries is a more reasonable approximation. Based on physical reasoning [16], the additional scattering time is given by

$$\tau_b(\omega)=\frac{W}{2|\mathbf{v}|\sin(\theta)}, \tag{17}$$

which represents the time required by the phonon to traverse a ribbon of width W. Provided this scattering mechanism is independent of the homogeneous scattering rate, the two can be combined using Matthiessen's rule. However, boundary scattering does not occur homogeneously throughout the ribbon as this approach assumes. Despite the above, this approach, labeled "Scat. rate" in Fig. 2, has been widely used in the literature and is significantly closer to the exact solution, which we now discuss.

Analytical Solution For Long Nanoribbons

Both of the above approximate approaches are unnecessary because the Boltzmann equation can be solved exactly for an infinitely long nanoribbon with diffuse boundaries. The solution given below is similar to the well-known classical size-effect of a thin film [9, 16, 21], but to our knowledge, has yet to appear in the literature for two-dimensional materials.

Using the fact that for this problem the distribution at the diffuse boundaries is at the local equilibrium, the solution for the distribution function for $0<\theta<\pi$ is [20]

$$f^{\mathrm{d}}(y)^{+}=-\tau|\mathbf{v}|\cos(\theta)\frac{\partial f^{\mathrm{BE}}}{\partial T}\frac{\mathrm{d}T}{\mathrm{d}x}\left(1-\exp\left(-\frac{y}{\tau|\mathbf{v}|\sin(\theta)}\right)\right) \tag{18a}$$

and for $\pi<\theta<2\pi$

$$f^{\mathrm{d}}(y)^{-}=-\tau|\mathbf{v}|\cos(\theta)\frac{\partial f^{\mathrm{BE}}}{\partial T}\frac{dT}{dx}\left(1-\exp\left(-\frac{(y-W)}{\tau|\mathbf{v}|\sin(\theta)}\right)\right) \tag{18b}$$

With the distribution function known, the effective ribbon conductivity can be calculated from Eqn. (8) and the error associated with the two above-described approximate approaches can be quantified. Fig. 2 shows that, as expected, the additional homogeneous scattering rate provides a better approximation than the frequency cut-off approach, but it still differs from the analytical solution by an error on the order of $5-10\%$.

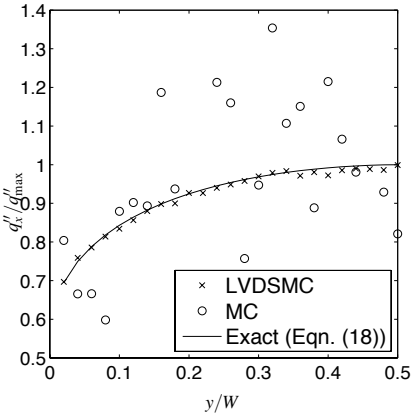

FIGURE 3. HEAT FLUX DISTRIBUTION ACROSS RIBBON. COMPARISON OF STANDARD MC AND LVDSMC.

Although the exact solution (18a) and (18b) is the "most efficient" solution to this specific problem, there are many more geometries for which no analytical solution is available. Thus the nanoribbon case serves to validate the LVDSMC method, which can then be used for problems less tractable by analytic approaches. As reflected in Fig. 2, the LVDSMC method is within 0.5% of the exact solution for all ribbon widths.

An important feature of both the exact solution and the LVDSMC method is that they can provide information about the spatial distribution of heat flux within a nanoribbon, while the approximate solutions are constrained to only the average heat flux. Figure 3 shows that the heat flux across the ribbon width is non-uniform.

Figure 3 also demonstrates the variance-reduction provided by the LVDSMC method compared to the standard direct Monte Carlo (MC) method. Both were run with essentially the same number of samples and computational cost. For a simulation domain of $L=6\mu m$, a temperature difference of 2K and $W=6\mu m$, the standard deviation in the heat flux obtained by LVDSMC is nearly two orders of magnitude smaller than the standard deviation of the MC solution (heat fluxes in the MC simulation were shifted to compensate for numerical issues with the MC approach); this corresponds to a speedup of almost four orders of magnitude (the standard deviation scales with the square root of the number of samples). As has been shown elsewhere [8, 9], the comparative advantage of the LVDSMC simulation continues to grow for smaller deviations from equilibrium. Determination of the effective conductivity of a structure at a specific temperature is inherently a small deviation from equilibrium problem, so this

feature is very valuable in this context.

CONCLUSION

The low-variance deviational Monte Carlo method allows efficient solution of thermal transport problems in graphene nanostructures and is significantly more efficient than the standard MC method for solving the Boltzmann equation. As a Monte Carlo based simulation method, it is easy to extend to more complicated geometries, which should be useful for investigating various features of thermal transport in graphene, as well as for designing and optimizing future graphene devices. A drawback of the present approach is the use of the relaxation time approximation for which only isotropic relaxation times are available. This imposed assumption of isotropy restricts us from conducting a consistent investigation of the effect of edge chirality in graphene nanoribbons.

An analytical solution for thermal transport in infinitely long graphene nanoribbons shows that the prominent approximate method for estimating the effective thermal conductivity is reasonable, and exhibits errors for the effective thermal conductivity on the order of 10%. The other frequently used approximation, based on a length scale cutoff, results in significantly larger errors. Finite-length nanoribbons do not lend themselves to analytical solutions and will be investigated in the future using low-variance deviational simulations.

ACKNOWLEDGMENT

The authors gratefully acknowledge financial support by the National Science Foundation Graduate Research Fellowship Program, the National Defense Science and Engineering Graduate Fellowship, and the MIT-Singapore Alliance. We are also grateful to Jean-Philippe Péraud for his helpful insights.

REFERENCES

[1] Das Sarma, S., Adam, S., Hwang, E. H., and Rossi, E., 2011. "Electronic transport in two dimensional graphene". *Rev. Mod. Phys.,* ***83***(2), pp. 407–470.

[2] Balandin, A. A., 2011. "Thermal properties of graphene and nanostructured carbon materials". *Nat. Mater.,* ***10***, pp. 569–581.

[3] Peierls, R., 1929. "On the kinetic theory of thermal conduction in crystals". *Ann. Phys.,* ***3***, pp. 1055–101.

[4] Hwang, E. H., and Das Sarma, S., 2008. "Acoustic phonon scattering limited carrier mobility in two-dimensional extrinsic graphene". *Phys. Rev. B,* ***77***(11), p. 115449.

[5] Baker, L. L., and Hadjiconstantinou, N. G., 2005. "Variance reduction for Monte Carlo solutions of the Boltzmann equation". *Phys. Fluids,* ***17***, p. 051703.

[6] Hadjiconstantinou, N. G., Garcia, A., Bazant, M., and He, G., 2003. "Statistical error in particle simulations of hydrodynamic phenomena". *J. Comput. Phys.,* ***187***, pp. 274–297.

[7] Homolle, T. M. M., and Hadjiconstantinou, N. G., 2007. "A low-variance deviational simulation Monte Carlo for the Boltzmann equation". *J. Comput. Phys.,* ***226***(2341-2358).

[8] Radtke, G. A., Hadjiconstantinou, N. G., and Wagner, W., 2011. "Low-noise Monte Carlo simulation of the variable hard-sphere gas". *Phys. Fluids,* ***23***, p. 030606.

[9] Péraud, J.-P. M., and Hadjiconstantinou, N. G., 2011. "Efficient simulation of multidimensional phonon transport using energy-based variance-reduced Monte Carlo formulations". *Phys. Rev. B,* ***84***, p. 205331.

[10] Bird, G. A., 1994. *Molecular Gas Dynamics and the Direct Simulation of Gas Flows*. Clarendon Press.

[11] Hao, Q., Chen, G., and Jeng, M.-S., 2009. "Frequency-depdendent Monte Carlo simulation of phonon transport in two-dimensional porous silicon with aligned pores". *J. Appl. Phys.,* ***106***, p. 114321.

[12] Klemens, P. G., 2001. "Theory of thermal conduction in thin ceramic films". *Int. J. Thermophys.,* ***22***(1), pp. 265–275.

[13] Nika, D. L., Ghosh, S., Pokatilov, E. P., and Balandin, A. A., 2009. "Lattice thermal conductivity of graphene flakes: Comparison with bulk graphite". *Appl. Phys. Lett.,* ***94***, p. 203103.

[14] Nika, D. L., Pokatilov, E. P., and Balandin, A. A., 2011. "Theoretical description of thermal transport in graphene: The issues of phonon cut-off frequencies and polarization branches". *Phys. Status Solidi B,* ***248***(11), pp. 2609–2614.

[15] Callaway, J., 1959. "Model for lattice thermal conductivity at low temperatures". *Phys. Rev.,* ***113***(4), pp. 1046–1051.

[16] Ziman, J. M., 1960. *Electrons and Phonons*. Oxford Clarendon Press.

[17] Aksamija, Z., and Knezevic, I., 2011. "Lattice thermal conductivity of graphene nanoribbons: Anisotropy and edge roughness scattering". *Appl. Phys. Lett.,* ***98***, p. 141919.

[18] Mounet, N., and Marzari, N., 2005. "First-principles determination of the structural, vibrational and thermodynamic properties of diamond, graphite, and derivatives". *Phys. Rev. B,* ***71***(20), p. 205214.

[19] Morelli, D. T., and Heremans, J. P., 2002. "Estimation of the isotope effect on the lattice thermal conductivity of group IV and group III-V semiconductors". *Phys. Rev. B,* ***66***, p. 195304.

[20] Landon, C. D., and Hadjiconstantinou, N. G., Submitted. "Phonon transport in graphene nanoribbons". *Phys. Rev. B*.

[21] Chen, G., 2005. *Nanoscale Energy Transport and Conversion*. Oxford University Press.